Nanotechnology **20** (2009) 135606 (7pp) doi:10.1088/0957-4484/20/13/135606

Single-walled carbon nanotubes decorated with a pyrene–fluorenevinylene conjugate

D Tasis[1], J Mikroyannidis[2], V Karoutsos[1], C Galiotis[1,3] and K Papagelis[1,4]

[1] Department of Materials Science, University of Patras, 26504 Rio Patras, Greece
[2] Department of Chemistry, University of Patras, 26504 Rio Patras, Greece
[3] Foundation for Research and Technology Hellas, Institute of Chemical Engineering and High Temperature Chemical Processes (FORTH—ICE/HT), 26504 Patras, Greece

E-mail: kpapag@upatras.gr

Received 5 January 2009, in final form 8 January 2009
Published 11 March 2009
Online at stacks.iop.org/Nano/20/135606

Abstract
Single-walled carbon nanotubes are noncovalently functionalized using a pyrene–fluorenevinylene dye and the resulting nanohybrids are isolated from the free molecules. The tubes modified by means of this noncovalent approach show enhanced solubility in organic media. The structure and morphology of this hybrid material are fully characterized using absorption, infrared and Raman spectroscopies as well as atomic force and scanning electron microscopies. Steady state fluorescence measurements reveal that significant quenching of the pyrene derivative excited state takes place through an energy transfer mechanism.

S Supplementary data are available from stacks.iop.org/Nano/20/135606

1. Introduction

Nanometre scale structures are of increased interest for the development of optoelectronic applications. Among the novel nanomaterials that have exerted a potential impact on technological issues, carbon nanotubes (CNTs) stand out owing to their extraordinary structural and electronic properties [1]. However, CNTs are almost insoluble to any aqueous and/or organic medium; most often they exist as bundles due to the van der Waals interactions between the graphitic sidewalls. Thus, the manipulation of the carbon nanostructures and their implementation in electronic devices is a difficult task which can often be alleviated by sidewall chemical modification [2].

One of the general approaches used to prepare individually dispersed tubes in solution involves the covalent functionalization of CNT sidewalls and tips [2]. However, such functionalization alters appreciably the electronic properties of the tubes by breaking their extended conjugation [3]. On the other hand, the noncovalent functionalization interferes slightly with the properties of CNTs, and thus it can be considered as the best strategy for exploiting their inherent electronic properties. In most cases, the CNT noncovalent functionalization can be achieved by adhesion of small molecules such as polycyclic aromatic compounds [4–12], helical wrapping of conjugated polymers [13–19] and stacking of porphyrins [20]. These aromatic systems interact with the surface of CNTs through π–π interactions, exfoliating partially the bundles and/or bringing individual tubes into solution.

Ideally, for electronic applications, it will be desirable to disperse and manipulate CNTs with suitable substances that can complement or enhance the inherent properties of the carbon nanomaterial. Conjugated polymers of general formula –Ar–C=C– are promising candidates as active components in light emitting diodes, photovoltaic cells and field-effect transistors. Oligomers are of particular interest because they generally possess good molecular ordering properties and they show enhanced solubility in organic media with the introduction of proper chemical substituents. Typical examples include oxadiazolephenylenevinylene and fluorenevinylene systems [21, 22]. The fascinating properties of luminescent conjugated oligomers originate from their curved tweezer-like structure and extended electron delocalization.

To our knowledge, the chemical interaction of CNTs by luminescent oligomers has not been studied in depth. Feng *et al* [21] have first studied the fluorescence quenching of 2,5-bis{3-[3-vinyl-9-(α-naphthyl)carbazolyl]phenyl}-1,3,4-

[4] Author to whom any correspondence should be addressed.

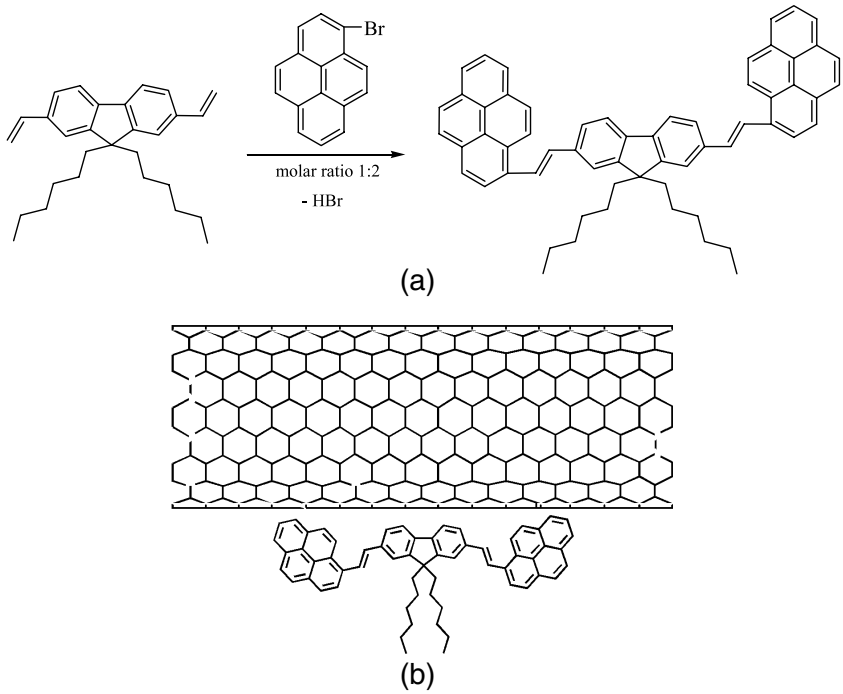

Figure 1. (a) Synthetic scheme of compound PFP, (b) adsorption of PFP trimer onto the SWCNT sidewalls.

oxadiazole oligomer (VNCO) by CNTs through titration studies, but the authors did not conduct full spectroscopic investigation of the interaction mode between the components.

Analogous electroactive systems, fluorenevinylene-based oligomers, could be ideal candidates for altering the CNT electronic properties, since they have demonstrated enhanced electroluminescent properties due to their strong blue-green fluorescence [22]. For this purpose, we have used a novel fluorescent organic compound (denoted as PFP) which contains a central 2,7-fluorenevinylene unit with two pyrenes attached at both sides (figure 1). The use of pyrene moieties is particularly crucial to achieve locking of the bifunctional dye onto CNT sidewalls through directed π–π interactions. In addition, the presence of two hexyl chains at the C-9 of fluorene give rise to enhanced dispersibility of the complexes.

We present here a detailed spectroscopic investigation that sheds light onto the interaction between the carbon nanostructures and the luminescent substance. A series of physicochemical probes (spectroscopic and microscopic) confirm electronic interactions between the fluorenevinylene–pyrene molecule and the CNTs.

2. Experimental details

2.1. Preparation of supramolecular complexes of CNTs with the dye

The synthesis and characterization of PFP derivative was described in an earlier work [22]. Briefly, PFP was synthesized by Heck coupling of 9,9-dihexyl-2,7-divinylfluorene with 3-bromopyrene in a molar ratio 1:2 according to figure 1(a). This reaction took place in N,N-dimethylformamide and triethylamine was used as acid acceptor.

As-received purified HiPco single-walled CNTs (SWCNTs) were acquired by Carbon Nanotechnologies, Inc., while their purity was ∼92% (diameter distribution between 0.8 and 1.2 nm). A small amount of the carbon material (2.5 mg) was dispersed in tetrahydrofuran (THF) by ultrasonic treatment for 1 h at room temperature and then left for 30 min for settling. We took only the upper part of the suspension in which the content of debundled tubes was relatively high compared to the lower part. A solution of PFP in THF was separately prepared and added to the well-dispersed CNT solution. The weight ratio between CNTs and PFP in the final suspension was set about 1:10, which was estimated by optical measurements. Bath sonication was continued for an extra period of 3 h. The solution was centrifuged at 3500 rpm for 10 min and the supernatant part with the excess of PFP was discarded. After extensive rinsing with THF, the functionalized CNT material was collected by filtration through hydrophobic membrane filter having 0.45 μm pore size.

2.2. Measurements

The UV/vis–NIR absorption spectra of the CNT samples in THF were recorded on a Digilab Hitachi U-2800 spectrophotometer. The FT-IR spectra were recorded on a Excalibur Digilab spectrophotometer, while the samples were prepared by the KBr pellet method.

The morphology of the CNT samples was revealed by atomic force microscopy (AFM) images recorded via a multimode scanning probe microscope (Digital Instruments). AFM tapping mode with the constant force method has been used. A standard 120 μm × 120 μm magnet-free scanner with vertical range 5 μm and z-axis resolution 0.05 nm has been utilized. The scan rate was 1 Hz. The cantilevers were

V shaped with spring constants 40 N m^{-1}. The shape of the silicon nitride tips was square pyramidal with radius of curvature ∼10 nm and half angle ∼15°. For the preparation of the samples, a THF suspension was sonicated for 1 h. One drop of the suspension was spin casted on a mica surface.

The scanning electron microscopy (SEM) observations were made on a Leo 1530 FESEM Gemini scanning microscope. THF suspensions of SWCNTs were spin casted on mica substrates. All specimens were sputtered with gold.

Raman spectra at ambient conditions were recorded by means of two different experimental setups. A micro-Raman setup collecting data in the back-scattering geometry and equipped with a triple monochromator and Peltier cooled CCD detector system. The 514.5 nm line of an Ar+ laser was used for excitation. The laser line was focused on the sample by means of a 50× objective with a spatial resolution of ∼2 μm, while the beam intensity was kept at ∼0.25 mW. Concerning the second setup, Raman spectra were acquired on a Renishaw inVia Raman system. The laser beam was focused on the sample with a 50× objective, while the 785 nm line from a diode laser was used for excitation at a power of ∼2 mW on the sample.

Room temperature photoluminescence (PL) spectra were obtained with a Perkin Elmer LS45 luminescence spectrometer. The PL spectra were recorded by using an excitation wavelength of 400 nm.

3. Results and discussion

3.1. Colloidal stability

The solubilization/dispersion of raw SWCNTs in THF containing PFP was carried out by using the typical procedure described in section 2. After the sonication period, the CNT/PFP suspension was centrifuged at 3500 rpm and rinsed extensively in order to remove the excess of the non-adsorbed PFP molecules. Optical measurement of the discarded supernatant solution showed that there was just a trace quantity of CNT material in that sample (optical density at 600 nm was ∼0.01). By applying a short-time sonication to the precipitated CNT material by using THF as a solvent, a stable suspension was formed. The resulting solutions were stable for periods exceeding one month. By optical measurements, the solubility of the supramolecular complex in THF was estimated to be about 0.8 mg ml^{-1}. Even after some precipitation due to solution concentration change, the SWCNT material could be redispersed by sonication for a relatively short time. The mechanism of PFP-induced solubilization of SWCNTs could be attributed to the combination of two factors. Firstly, the extended conjugation of PFP results in a semi-rigid curved structure which favours the adsorption onto SWCNT sidewalls. Moreover, the presence of aliphatic chains in the fluorene moiety gives rise to an enhanced dispersibility of the supramolecular complexes in organic media.

3.2. Microscopy imaging

Morphological AFM images of the SWCNT material functionalized by PFP are shown in figure 2. The tubes

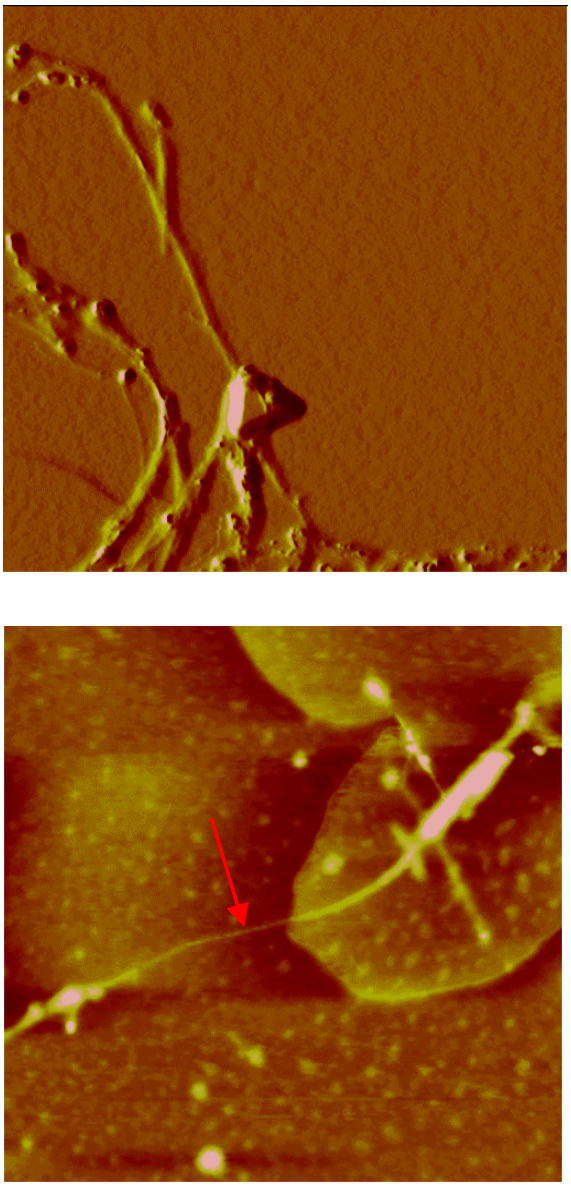

Figure 2. AFM images of PFP-modified SWCNT material. The arrow points to individual SWCNTs.
(This figure is in colour only in the electronic version)

are not homogeneously wrapped by the oligomer; some regions are coated by an amorphous PFP layer, due to the tendency of pyrene derivatives to form aggregates, while others seems to be unmodified or covered by an organic monolayer. The pyrene stacking interactions explain why the colloidal stability of the CNT hybrid in THF shows some time dependency. The calculated height value for the designated part of the nanostructure in the bottom image of figure 2 was 1.34 nm, typical of individual single-walled nanotube diameter. This clearly indicates the existence of individually dissolved SWCNTs in solution, since the diameter of the HiPco tubes is 0.8–1.2 nm. Nevertheless, bundled tubes were also observed in the AFM images; that is, the heights of the nanostructures were estimated to be more than 5 nm.

These observations indicate that the oligomer chains have spontaneously adsorbed onto the SWCNTs. Evidently,

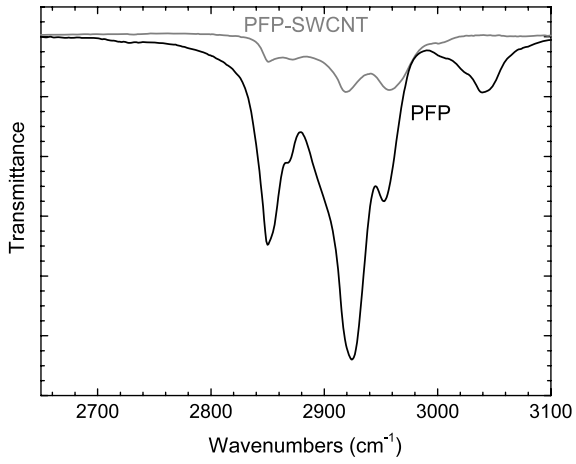

Figure 3. FT-IR transmittance spectra of neat pyrene derivative and hybrid material.

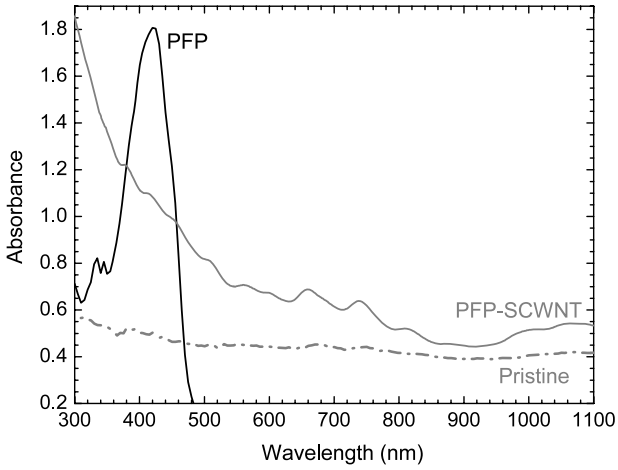

Figure 4. Absorption spectra of pristine HiPco SWCNTs, free 2,7-fluorenevinylene derivative and the hybrid material in THF solutions.

the adsorption process has made the tubes soluble in the organic solvent. To further examine the stacking of the oligomer chains around the SWCNT sidewalls, we cast thin films of the hybrids on mica substrates from PFP-modified SWCNT solutions. The morphology of the nanostructures was checked by SEM. As can be seen from figure S1a included in the supporting information (available at stacks.iop.org/Nano/20/135606), the SEM image of pristine SWCNT material reveals densely entangled networks, indicating that the unmodified nanostructures self-aggregate to form large bundles. On the contrary, the hybrid material is featured by thin ropes clothed with organic material (figure S1b (available at stacks.iop.org/Nano/20/135606)).

3.3. UV–vis and infrared spectroscopies

The presence of PFP onto the SWCNT sidewalls was also supported by FT-IR (figure 3). As shown, the neat pyrene derivative exhibits four main peaks in the range of 2500–3100 cm^{-1}. The appearance of the peaks situated at 2855, 2925, 2960 and 3040 cm^{-1} indicates the existence of C–H bonds in both aliphatic and aromatic systems. Specifically, the absorption bands at 2855, 2925 and 2960 cm^{-1} are assigned to the C–H stretching of the hexyl side chains, while the absorption band at 3040 cm^{-1} is associated with the aromatic rings. In the case of SWCNT–PFP hybrid spectrum, the main characteristic peaks of the pyrene derivative coexist, while that of the 3040 cm^{-1} peak is attenuated dramatically. These results suggest that a strong interaction between the adsorbed PFP and SWCNTs takes place. The rather weak PFP signals in the spectrum of the hybrid may reflect the degree of loading of adsorbed pyrene derivative onto CNT sidewalls.

The exohedral noncovalent attachment of the organic substance and the subsequent dispersion of SWCNT material in THF solutions were made evident by utilizing the UV–visible/Near-IR spectroscopy (figure 4). The spectrum of neat pyrene derivative showed an intense feature located at ∼420 nm, while above 500 nm the absorption coefficient was diminished appreciably. The starting SWCNT material exhibited poorly resolved van Hove singularities, whereas the absorption spectrum of the composite reveals well defined transitions. This indicates that the tubes are present as individuals and/or as partially debundled due to the binding of pyrene molecules onto the SWCNT graphitic sidewalls. Concerning the intensities of the spectra in the visible region, the spectrum of PFP-modified SWCNTs exhibits a higher absorbance in the range 300–800 nm when compared to the one of the unmodified tubes. The opposite trend was observed in a study by Fernando *et al* [6], where CNT material showed diminished band gap transitions after complexation with a pyrene derivative. Yet, the conditions used for recording the reference UV–vis spectra of unmodified tubes is slightly different in both cases, as Fernando *et al* used a CNT/surfactant aqueous solution, whereas we show the spectrum of neat SWCNTs in THF. Although PFP absorbs in a part of this spectral range, we attribute the enhanced absorbance to the formation of a complex between the pyrene derivative and SWCNTs [23].

3.4. Fluorescence spectroscopy

Support for the π–π interaction between SWCNTs and PFP was obtained from photophysical studies (figure 5). Under dilute THF solutions, PFP showed intense monomer fluorescence with maximum at 471 nm. An additional peak at 500 nm was attributed to emission by excited PFP aggregates (excimers) [22]. The fluorescence quantum yield (Φ_f) was estimated about 74%, whereas a significant emission quenching ($\Phi_f = 2.8\%$) was observed for the CNT–PFP composite material (a solution of quinine sulfate which has $\Phi_f = 54.6\%$ was used as a standard). Analogous trends were observed in other noncovalently linked SWCNT/pyrene derivatives [10, 11]. Due to the relatively high ionization potential of PFP (5.75 eV) [22], the photoluminescence quenching of pyrene singlet excited state by SWCNTs was attributed to the efficient energy transfer between PFP and tubes, rather than electron transfer or disruption of π-conjugation caused by a conformational change. Energy

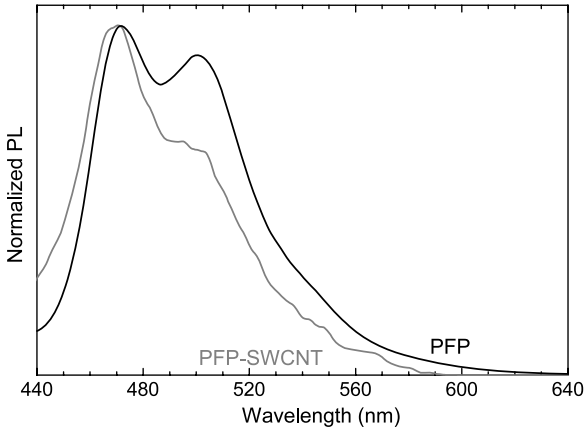

Figure 5. Normalized fluorescence spectra of neat pyrene derivative and modified SWCNT material.

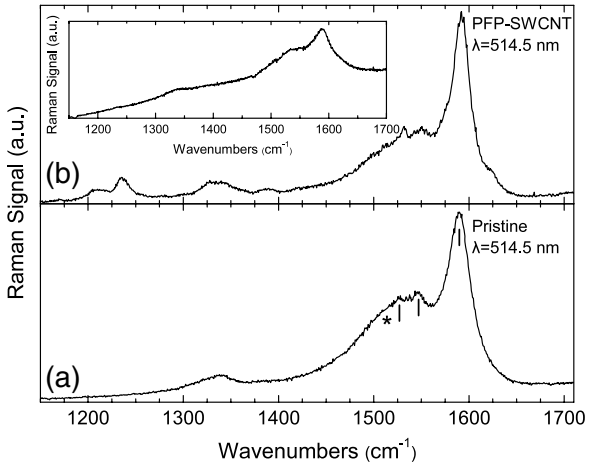

Figure 6. Tangential bands in typical Raman spectra for (a) as produced HiPco SWCNTs and (b) PFP-SWCNT material, recorded with the 514.5 nm excitation energy. Vertical lines denote the main G-band components while the asterisk indicates the location of the G^- (BWF) component of the metallic SWCNTs. The inset shows the Raman spectrum of PFP-SWCNT hybrid containing an excess of pyrene derivative.

transfer quenching between molecules and for molecules on graphitic carbon is well known [24].

3.5. Raman

Raman spectroscopy is a particularly useful experimental technique to probe sensitively the noncovalent interactions between CNTs and various molecular moieties. Figure 6 shows the room temperature Raman spectra for the pristine and modified SWCNT material in the tangential mode region, using the 514.5 nm (2.41 eV) excitation. According to the Kataura plot [25], the use of such wavelength enhances predominantly the Raman signal from the metallic SWCNTs. For the pristine material four features constitute the tangential band, located at 1512, 1526, 1548 and 1590 cm^{-1}. The lower frequency broad component at 1512 cm^{-1} (marked with asterisk) is the asymmetric Breit–Wigner–Fano (BWF) type G-peak of the metallic tubes ($|1/q| = 0.1$, $\Gamma = 60.5$ cm^{-1}), while the higher frequency one at 1590 cm^{-1} is attributed to the G^+ component of both metallic and semiconducting nanotubes. Moreover, the bands at 1526 and 1548 cm^{-1} should be associated with the diameter dependent G^- component of the larger diameter metallic tubes and the smaller diameter semiconducting tubes, respectively [26].

In addition, the inset presents the Raman spectrum of PFP-SWCNT hybrid containing an excess of pyrene derivative. In this case, the characteristic Raman features were poorly resolved due to a luminescence background originated from the tail of the PFP absorption band (figure 4). The successful removal of the free pyrene derivative molecules can be clearly observed from the spectrum of PFP–SWCNT in figure 6(b). By comparing with the spectrum of pristine tubes, the additional peaks in figure 6(b) for PFP-SWNT material are assigned to the Raman response of the pyrene derivative itself. Furthermore, contribution in the spectral intensity of the tangential band should be expected. The G^+ peak of the PFP–SWCNT exhibits a small blue shift of 2 cm^{-1} and becomes narrower compared to the pristine one. The full width at half maximum (FWHM) is decreased from 25.1 cm^{-1} for PFP–SWCNT to 21 cm^{-1} for the pristine sample. Moreover, upon noncovalent modification the G^+ peak intensity relative to the rest tangential components increase significantly suggesting the presence of individual tubes and/or thin bundles [27, 28]. This behaviour is similar to that reported by Stepanian *et al* [29] for pyrene-modified samples indicating complex formation between the aromatic modifiers and the nanotube sidewalls.

The Raman spectra of pristine and SWCNT–pyrene derivative complex recorded for the G-band region with excitation of 785 nm is shown in figure S2 (supporting information (available at stacks.iop.org/Nano/20/135606)). Spectral deconvolution by fitting multiple Lorentzian fits, is indicated by the solid lines in figure S2 (available at stacks.iop.org/Nano/20/135606); the constituent peak positions are also shown. The SWCNTs that are resonant with the 785 nm (1.58 eV) are predominantly semiconducting and resonant with the $E_{22}(S)$ interband transition energy. Similarly to that observed for the $\lambda_{exc} = 514.5$ nm, the longitudinal tangential vibration G^+ peak at 1590 cm^{-1} becomes narrower (from 13 cm^{-1} for the pristine to 11 cm^{-1} for the hybrid material) and the intensity of the circumferential tangential G-components becomes weaker relative to the G^+ peak, after the noncovalent functionalization. This further supports the effective exfoliation of pristine SWCNT bundles due to the sonication-assisted decoration of SWCNT sidewalls.

Figure 7 depicts the radial breathing modes (RBMs) for the pristine and PFP-SWCNT samples using the 514.5 and 785 nm excitation wavelengths. The frequency positions of the main peaks obtained with Lorentzian lineshapes are also shown. Aggregation due to the strong intertube interaction within the bundles broadens the SWCNT resonance windows (from ∼40 to ∼200 meV in some cases) downshifting their interband electronic transition energies and changing their effective Raman excitation profile [30]. In particular, RBMs of SWCNTs are highly sensitive to their aggregation state. For $\lambda_{exc} = 785$ nm, the peak at 233 cm^{-1} assigned to

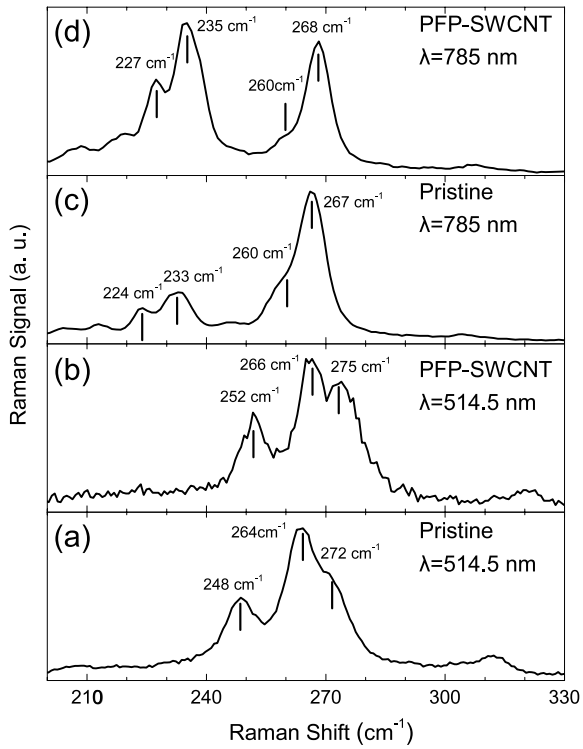

Figure 7. RBM Raman spectra at room temperature for pristine SWCNTs and PFP-SWCNT material excited with the 514.5 and 785 nm.

the (10, 5) tube [28] is off resonance in the pristine sample and comes into resonance with the $E_{22}(S)$ transitions of the hybrid material. Those changes are consistent with the downshifting and broadening of the corresponding transitions in the aggregate state. Furthermore, the intensity of the peak at 267 cm^{-1}, assigned to the (10, 2) tube, diminishes for individually dispersed HiPco nanotubes [30]. This peak in PFP-SWCNT sample loses intensity relative to the cluster of peaks around 230 cm^{-1} indicating the presence of thin bundles in the studied sample [30] due to pyrene/SWCNTs stacking interactions. Moreover, the peaks located at 233 and 267 cm^{-1} for the pristine sample shift to 235 and 268 cm^{-1}, respectively, for the hybrid material. This indicates that SWCNTs become stiffer after coated with the PFP molecules, due to the π–π interactions. This mode hardening effect is also observed in the case of polycyclic aromatic hydrocarbons [31]. Similar behaviour is observed for $\lambda_{exc} = 514.5$ nm whereas the RBM peaks around 260 cm^{-1} upshift upon CNT modification (figure 7).

4. Conclusion

We have described the importance of a novel pyrene–fluorenevinylene conjugate for the noncovalent functionalization and dispersion of CNT material. Moreover, the presence of aliphatic pendant groups plays an important role in the solubilization process of the hybrid material in organic media. Organic solutions of the supramolecular complex exhibited interesting fluorescence properties. The efficient fluorescence quenching of the physisorbed pyrene chromophore suggested energy transfer from the pyrene group to the SWCNTs.

UV–vis and Raman spectroscopies strongly support the effective exfoliation of CNT bundles due to the sonication-assisted decoration of CNT sidewalls by PFP moieties. The application of such energy transfer hybrid materials can be expanded further in many fields of electronic nanodevices.

Acknowledgment

This work was supported by a ‘K. KARATHEODORIS’ grant from the University of Patras Research Committee, Patras, Greece.

References

[1] Sgobba V, Rahman G M A, Ehli C and Guldi D M 2006 Covalent and noncovalent approaches towards multifunctional carbon nanotube materials *Fullerenes* (*RSC Nanoscience and Nanotechnology Series*) ed F Langa de la Puente and J F Nierengarten (Cambridge: Royal Society of Chemistry)
[2] Tasis D, Tagmatarchis N, Bianco A and Prato M 2006 *Chem. Rev.* **106** 1105
[3] Aprile C, Martin R, Alvaro M, Scaiano J C and Garcia H 2008 *Chem.—Eur. J.* **14** 5030
[4] Chen R J, Zhang Y G, Wang D W and Dai H 2001 *J. Am. Chem. Soc.* **123** 3838
[5] Zhang J, Lee J K, Wu Y and Murray R W 2003 *Nano Lett.* **3** 403
[6] Shiral Fernando K A, Lin Y, Wang W, Kumar S, Zhou B, Xie S Y, Cureton L T and Sun Y P 2004 *J. Am. Chem. Soc.* **126** 10234
[7] Hedderman T G, Keogh S M, Chambers G and Byrne H J 2004 *J. Phys. Chem.* B **108** 18860
[8] Tomonari Y, Murakami Y H and Nakashima N 2006 *Chem.—Eur. J.* **12** 4027
[9] Ehli C *et al* 2006 *J. Am. Chem. Soc.* **128** 11222
[10] Zhang Y, Yuan S, Zhou W, Xu J and Li Y 2007 *J. Nanosci. Nanotechnol.* **7** 2366
[11] Ogoshi T, Takashima Y, Yamaguchi H and Harada A 2007 *J. Am. Chem. Soc.* **129** 4878
[12] Herranz M A, Ehli C, Campidelli S, Gutierrez S M, Hug G L, Ohkubo K, Fukuzumi S, Prato M, Martin N and Guldi D M 2008 *J. Am. Chem. Soc.* **130** 66
[13] Curran S A *et al* 1998 *Adv. Mater.* **10** 1091
[14] Star A, Stoddart J F, Steuerman D, Diehl M, Boukai A, Wong E W, Yang X, Chung S W, Choi H and Heath J R 2001 *Angew. Chem. Int. Edn* **40** 1721
[15] Chen J, Liu H, Weimer W A, Halls M D, Waldeck D H and Walker G C 2002 *J. Am. Chem. Soc.* **124** 9034
[16] Xu Z, Wu Y, Hu B, Ivanov I N and Geohegan D B 2005 *Appl. Phys. Lett.* **87** 263118
[17] Lee K W, Lee S P, Choi H, Mo K H, Jang J W, Kweon H and Lee C E 2007 *Appl. Phys. Lett.* **91** 023110
[18] Massuyeau F, Aarab H, Mihut L, Lefrant S, Faulques E, Wery J, Mulazzi E and Perego R 2007 *J. Phys. Chem.* C **111** 15111
[19] Yuan W Z, Mao Y, Zhao H, Sun J Z, Xu H P, Jin J K, Zheng Q and Tang B Z 2008 *Macromolecules* **41** 701
[20] Murakami H, Nomura T and Nakashima N 2003 *Chem. Phys. Lett.* **378** 481

[21] Feng L and Chen Z 2006 *Spectrochim. Acta* A **63** 15
[22] Mikroyannidis J A, Fenenko L and Adachi C 2006 *J. Phys. Chem.* B **110** 20317
[23] Paloniemi H, Aaritalo T, Laiho T, Like H, Kocharova N, Haapakka K, Terzi F, Seeber R and Lukkari J 2005 *J. Phys. Chem.* B **109** 8634
[24] Kagan M R and McCreery R L 1994 *Anal. Chem.* **66** 4159
[25] Kataura H, Kumazawa Y, Ohtsuka Y, Suzuki S, Maniwa Y and Achiba Y 1999 *Synth. Met.* **103** 2555
[26] Kawamoto H, Uchida T, Kojima K and Tachibana M 2006 *J. Appl. Phys.* **99** 094309
[27] Liu Y, Gao L, Zheng S, Wang Y, Sun J, Kajiura H, Li Y and Noda K 2008 *Nanotechnology* **18** 365702
[28] Karajanagi S S, Yang H, Asuri P, Sellitto E, Dordick J S and Kane R S 2006 *Langmuir* **22** 1392
[29] Stepanian S G, Karachevtsev V A, Yu Glamazda A, Dettlaff-Weglikowska U and Adamowicz L 2003 *Mol. Phys.* **101** 2609
[30] Ericson L M and Pehrsson P E 2005 *J. Phys. Chem.* B **109** 20276
[31] Gotovac S, Honda H, Hattori Y, Takahashi K, Kanoh H and Kaneko K 2007 *Nano Lett.* **7** 583